Synthesis and characterization of novel furoate azodye using spectral and thermal methods of analysis

Anca Moanta · Adriana Samide · P. Rotaru ·
Catalina Ionescu · B. Tutunaru

Abstract A new azoester, 4-(4-chloro-phenyldiazenyl)-2,6-dimethyl-phenyl 2-furoate (CPPF), has been synthesized by condensing 4-(4-chloro-phenylazo)-2,6-dimethyl-phenol with 2-furoyl chloride in pyridine. This compound has been characterized by elemental analysis (C, H, N), FTIR, UV–Vis, NMR (^{1}H and ^{13}C), and thermal analysis studies. Spectral analysis results confirmed the structure of the compound synthesized. Thermal analysis established that CPPF is stable up to 260 °C; melts at about 178 °C; and between 260 and 450 °C, it decomposes in two steps.

Keywords Azo dye · Thermal analysis · FTIR · UV–Vis · NMR

Introduction

The azo dyes represent a principal class of compounds with wide industrial applications where their thermal behavior is important to show the adequate range of temperature for that there are no risks to be used.

A. Moanta · A. Samide · C. Ionescu · B. Tutunaru
Department of Chemistry, Faculty of Mathematics and Natural Sciences, University of Craiova, 107i Calea Bucuresti, 200512 Craiova, Romania

P. Rotaru (✉)
Department of Physics, Faculty of Mathematics and Natural Sciences, University of Craiova, 13 A.I. Cuza Street, 200585 Craiova, Romania
e-mail: protaru@central.ucv.ro; petrerotaru@yahoo.com

In this direction, the research was recently oriented to study the thermal decomposition kinetics for a large series of aromatic azomonoether [1–5]. The thermal and electron impact decomposition of 4-hydroxy-4′-cyano-azobenzene were also investigated, knowing that its derivatives are used to synthesize the photo-responsive azobenzene polymers [6]. On the other hand, the possibility to obtain thin-film deposition by matrix-assisted pulsed laser evaporation of a 4CN-type azomonoether was investigated in association with thermal analysis [7].

Another interesting property of azomonoethers is represented by their liquid crystalline behavior that makes azomonoethers good candidates as liquid crystals for non-linear optics applications or for dye lasers. Thus, the synthesis and characterization of a new azomonoether dye with liquid crystalline properties were performed and reported in our previous study [8].

Recently, we have become interested in other useful applications of azo dyes, represented by their possible usage as corrosion inhibitors for carbon steel in various environments [9], and consequently a new synthesized azoester was reported as an effective inhibitor for carbon steel corrosion in saline water; this is being investigated using potentiodynamic polarization, electrochemical impedance spectroscopy (EIS), and X-ray photoelectron spectroscopy (XPS) [9–16].

As a continuation of our research, the aims of this study are focused on the synthesis and characterization of a new azo dye, namely 4-(4-chloro-phenyl diazenyl)-2,6-dimethyl-phenyl 2-furoate using specific methods such as FTIR, NMR (^{1}H and ^{13}C), and thermal analysis. CPPF is a potential inhibitor of corrosion.

Experimental

Synthesis of 4-(4-chloro-phenyldiazenyl)-2,6-dimethyl-phenyl 2-furoate (CPPF).
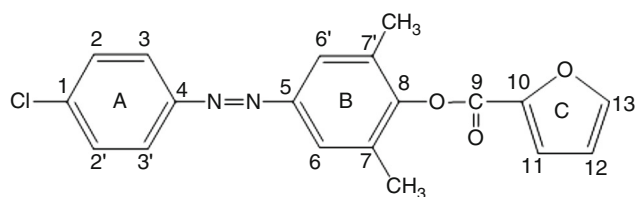
Fig. 1 Structure of CPPF and employed numbering system

4-(4-chloro-phenylazo)-2,6-dimethyl-phenol was synthesized by coupling the diazonium salt of 4-chloro-aniline with 2,6-xylenol. The obtained azo compound was purified by recrystallization from ethanol, and its purity was examined by thin-layer chromatography and was checked by noting the melting points after successive recrystallizations. 4-Chloro-aniline,2,6-xylenol, pyridine, and 2-furoyl chloride used in the synthesis were Aldrich products.

CPPF was obtained by a coupling reaction between 4-(4-chloro-phenylazo)-2,6-dimethyl-phenol and 2-furoyl chloride in the presence of pyridine [9].

In a balloon equipped with reflux refrigerator, 1.7 g (6.52 mmol) of 4-(4-chloro-phenylazo)-2,6-dimethyl-phenol, 30 mL of pyridine, and 0.85 g (6.51 mmol) of 2-furoyl chloride were added. The obtained solution was mixed for 60 min at room temperature and then left to stand overnight, after which it was poured over 100 mL of distilled water. 2 mL of concentrated HCl-solution was then added, and the mixture was filtered using a G3 filter. The precipitate was washed with water and dried in the drying stove at 95 °C. The product was crystallized from ethanol to give the present compound of m.p. 177.5 °C with the yield of 79 %. The purity was checked by thin-layer chromatography ($Rf = 0.8$ toluene: acetone = 9:1). Elemental analysis values for the compound $C_{19}H_{15}N_2O_3Cl$ are as follows: calcd: C, 64.31; H, 4.23; N, 9.89 %; found: C, 64.17; H, 4.18; N, 9.65 %. The structure of the azoester is shown in Fig. 1.

Methods and technique

Elemental analysis of carbon, hydrogen, and nitrogen has been performed using a Carlo-Erba O/EA 1108 Analyzer.

Chemical bonding of the CPPF sample was investigated by FTIR with a PerkinElmer SPECTRUM100 Spectrometer in the wavenumber range of 650–4,000 cm^{-1}. The spectrum was obtained using universal attenuated total reflectance (UATR) accessory, at a resolution of 4 cm^{-1}, with 10 scans, and CO_2/H_2O correction.

The UV–Vis measurements have been carried out with a UV–Vis Varian Cary-50 Bio- spectrophotometer.

The NMR spectra were recorded on a Varian Gemini 300 Spectrometer, in CDCl$_3$ solution, working at 300 MHz for ^{1}H and 75 MHz for ^{13}C. The chemical shifts (δ) of ^{1}H and ^{13}C spectra are reported in ppm, with the ^{1}H and ^{13}C chloroform signals at 7.26 ppm and at 77.00 ppm, respectively. The coupling constants (J) are reported in Hz. Proton spectra have been described using the following abbreviations: s (singlet), d (doublet), dd (double doublet).

Thermal analysis measurements (TG, DTG, DTA, and DSC) of the CPPF compound were carried out in dynamic air atmosphere (150 cm^3 min^{-1}), under non-isothermal linear regimes, using a horizontal DIAMOND TG/DTA Analyzer from PerkinElmer Instruments, equipped with Pyris software.

Results and discussion

Spectral characterization of CPPF

FTIR spectrum

The FTIR spectroscopy is a widely used technique to determine the composition and structure of organic molecules and of the metal–organic complexes [17–21].
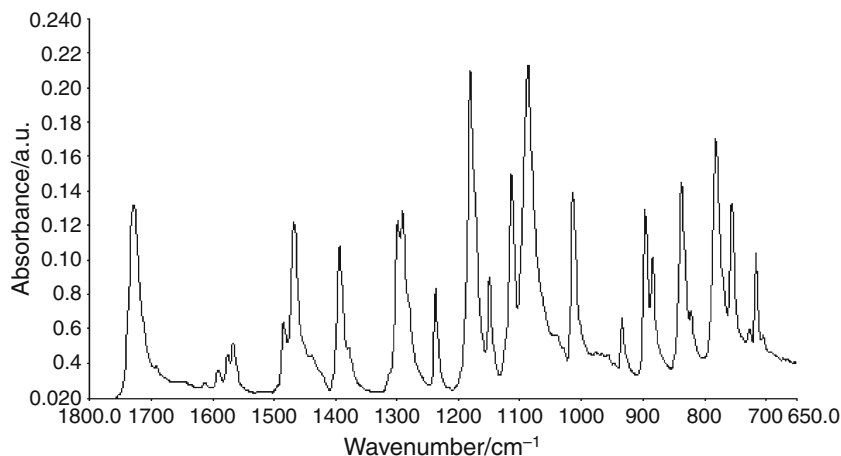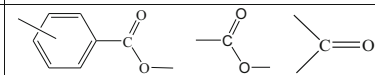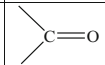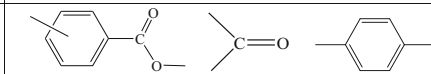
Fig. 2 FTIR spectrum of CPPF
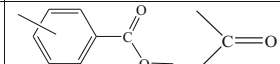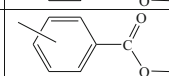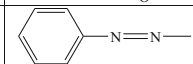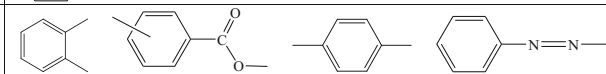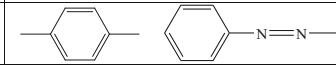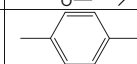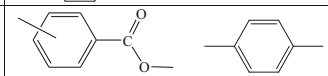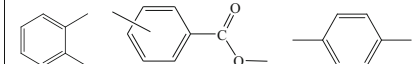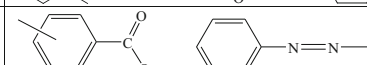
Table 1 Characteristic absorption bands for the individual groups of CPPF

Wavenumber (Intensity*)/cm^{-1}	Assignments
1728.13 (s), 1298.64 (s), 1290.89 (s), 1113.63 (s), 1086.60 (vs)	[chemical structure]
1612.76 (vw)	[chemical structure]
1590.65 (w)	[chemical structure]
1575.57 (w)	[chemical structure]
1566.35 (m)	[chemical structure]
1484.19 (m)	[chemical structure]
1466.94 (s)	[chemical structure]
1393.20 (s)	[chemical structure]
1236.92 (m), 1180.68 (vs), 1149.73 (m), 1014.60 (s)	[chemical structure]
933.92 (m), 896.22 (s), 884.20 (m)	[chemical structure]
837.16 (s)	[chemical structure]
781.76 (vs)	[chemical structure]
755.35 (s)	[chemical structure]
715.93 (m)	[chemical structure]

* *vs* very strong, *s* strong, *m* medium, *w* weak, *vw* very weak
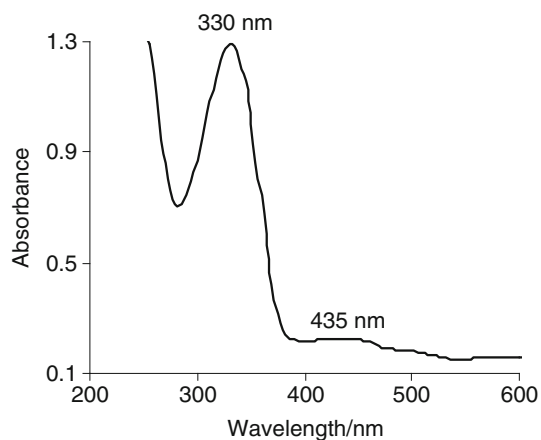
Fig. 3 UV–Vis spectrum of CPPF

FTIR spectrum in absorbance mode for CPPF is presented in Fig. 2, and the characteristic absorption bands for the individual functional groups are shown in Table 1. In Fig. 2 has been preserved only the range of 1,800–650 cm^{-1}, where CPPF has the most important absorption lines.

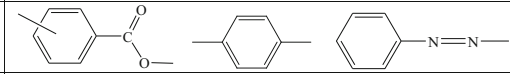Infrared absorption maxima into FTIR spectrum of CPPF have been attributed to functional groups, using the library of spectra of PerkinElmer SPECTRUM100 Spectrometer [8, 9, 18, 20]. The most intense absorption bands of CPPF, identified in the IR spectrum, were attributed to the following functional groups (chemical bonding):

– Absorption lines at 1484.19 (m), 1466.94 (s), 1393.20 (s), 781.76 (vs), and at 715.93 (m) cm^{-1} are related to azo group-linked benzene.

– Absorption lines at 1728.13 (s), 1590.65 (w), 1575.57 (w), 1566.35 (m), 1466.94 (s), 1298.64 (s), 1290.89 (s), 1113.63 (s), 1086.60 (vs), 837.16 (s), 781.76 (vs), and at 755.35 (m) cm^{-1} are related to carboxylic acid esters.

– Absorption lines at 1728.13 (s), 1590.65 (w), 1575.57 (w), 1298.64 (s), 1290.89 (s), 1236.92 (m), 1180.68 (vs), 1149.73 (m), 1113.63 (s), 1086.60 (vs), and at 1014.60 (s) cm^{-1} are related to carbonyl group.

– Absorption lines at 1590.65 (w), 1466.94 (s), 1393.20 (s), 933.92 (m), 896.22 (s), 884.20 (s), 837.16 (s), and at 781.76 (vs) cm^{-1} are related to aromatic compounds *para*-substituted.

– Absorption lines at 1466.94 (s) and at 755.35 (s) cm^{-1} are related to aromatic compounds *ortho*-substituted.

FTIR spectroscopy results confirm the existence of the main constituents in the CPPF molecule.

UV–Vis spectrum

A proof of CPPF structure is its electronic spectrum registered in dioxane solution prepared 24 h before the registration (Fig. 3).

The spectral analysis in UV–Vis shows absorption bands due to the main parts of this compound. The presence of such intense absorption K-bands at 330 nm, as a result of the conjugated system Ar–N=N–Ar, and low intensity R-bands at 435 nm, due to the –N=N– chromophore [22] can be noted.

The presence of R-band is due to n → π* transitions, which correspond to an electron transition from a pair of non-participant electrons of a heteroatom (N from azo group) on a non-bonding π* orbital, while that of K-band is due to electronic transitions between bonding and non-bonding orbitals, π → π* [22–24].

NMR spectra

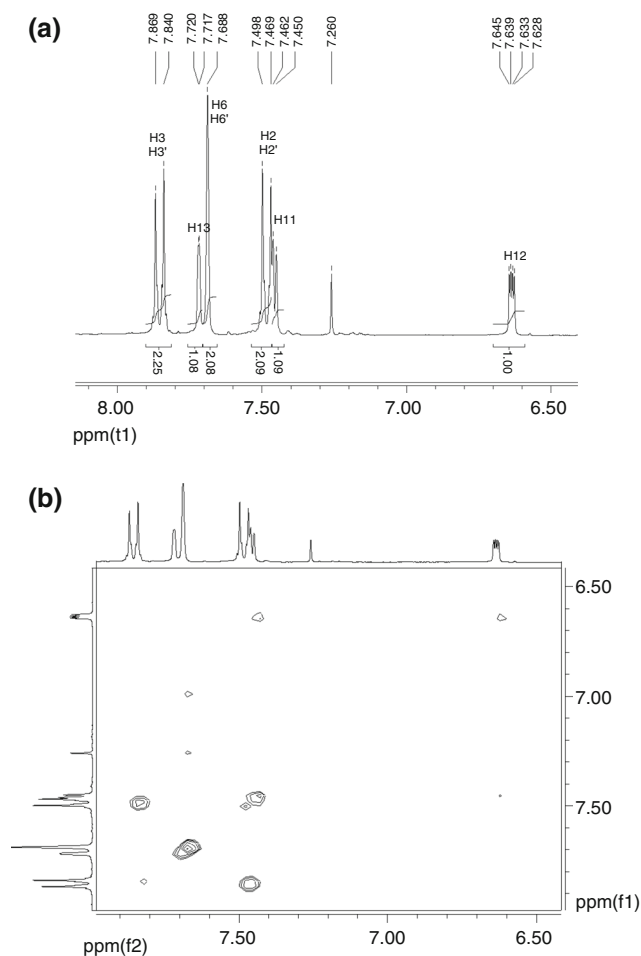The description of the NMR spectra of CPPF is realized in Figs. 4 and 5.

Fig. 4 **a** ^{1}H NMR spectrum of CPPF in CDCl$_3$- aromatic protons region only; **b** COSY(^{1}H-^{1}H) correlation spectrum of CPPF- aromatic protons region only
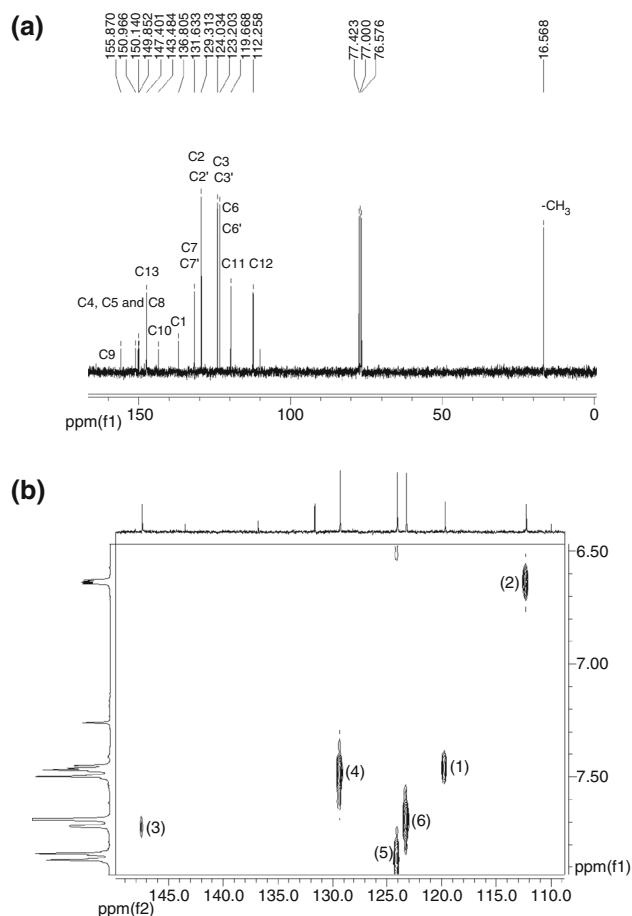

Fig. 5 **a** ^{13}C-NMR spectrum of CPPF in CDCl$_3$; **b** Hetero-correlation (^{1}H–^{13}C) spectrum of CPPF- aromatic atoms region only

Table 2 ^{1}H and ^{13}C NMR parameters of CPPF

^{1}H		^{13}C	
Atom	δ/ppm (multiplicity and coupling constants)	Atom	δ/ppm
–	–	C_1	136.8[a]
H_2 and $H_{2'}$	7.49 (AA' part of the AA'XX' system)	C_2 and $C_{2'}$	129.3
H_3 and $H_{3'}$	7.85 (XX' part of the AA'XX' system)	C_3 and $C_{3'}$	124.0
–	–	C_4	150.1[a,b]
–	–	C_5	151.0[a,b]
H_6 and $H_{6'}$	7.69 (s)	C_6 and $C_{6'}$	123.2
–	–	C_7 and $C_{7'}$	131.6
–	–	C_8	149.9[a,b]
–	–	C_9	155.9
–	–	C_{10}	143.5
H_{11}	7.46 (d, $^{3}J_{H11-H12} = 3.5$ Hz)	C_{11}	119.7
H_{12}	6.64 (dd, $^{3}J_{H12-H13} = 1.7$ Hz; $^{3}J_{H12-H11} = 3.5$ Hz)	C_{12}	112.3
H_{13}	7.72 (d, $^{4}J_{H13-H11} = 0.8$ Hz)	C_{13}	147.4
–CH_3	2.30 (s)	–CH_3	16.6

[a] These assignments were realized on the basis of calculations using additive substituent effects [22]

[b] These assignments may be interchanged

Fig. 4a shows that the signals belonging to the four protons from the disubstituted aromatic ring make up an [AA'XX'] system. The signals of H_2 and $H_{2'}$ protons are displayed at 7.49 ppm and those of H_3 and $H_{3'}$ at 7.85 ppm, with the azo group being a more *ortho* deshielding group than chlorine [25]. The coupling of these protons can be noticed in the bidimensional homo-correlation spectrum (Fig. 4b). The signals of ring B protons form two singlets,

one at 2.30 ppm, corresponding to the six protons of the two–CH_3 groups [22], and the second one being assigned to the two aromatic protons H_6 and $H_{6'}$, at 7.69 ppm [23]. Regarding ring C, the signal of H_{12} is displayed at 6.64 ppm and it is a double doublet, because H_{12} couples with both H_{11} and H_{13}, while H_{11} and H_{13} signals have doublets at 7.46 and 7.72 ppm, respectively [26].

The signals in ^{13}C NMR spectrum (Fig. 5a) have been assigned using subsistent additive effects [27] and the bidimensional hetero-correlation spectrum (Fig. 5b). Using this spectrum, C11, C12, and C13 could be precisely assigned, due to the correlation spots labeled (1), (2), and (3), respectively. Carbons C_2, $C_{2'}$ and C_3, $C_{3'}$ have been assigned to spots (4) and (5), while C_6 and $C_{6'}$ to spot (6). The results of these assignments are gathered in Table 2.

Thermal behavior of CPPF

Thermal analysis of some azoesters showed that dyes of this class of compounds are thermally stable at specific temperatures, sometimes presenting properties of liquid crystals [28–30].

The thermal stability of the CPPF determined by TA measurements, as well as the thermal effects, can be observed in the TG, DTG, DTA, and DSC curves in air dynamic atmospheres, at the heating rates (β) of 2, 4, 6, 8, and 10 K min^{-1}. Samples, of 2.452–4.655 mg, contained in aluminum crucibles, were heated in the temperature range of 20–600 °C. Of them in Fig. 6, we present only the curves obtained with β = 2 K min^{-1}, and for the remaining heating rates, the curves are being similar. DSC and DTA curves were found to be similar; in Fig. 6, only the DSC curve was represented, to calculate enthalpic effects.

CPPF is stable up to about 260 °C. Between 166.00 and 186.00 °C CPPF melts, the process being endothermic. Between 260 and 450 °C, oxidative decomposition

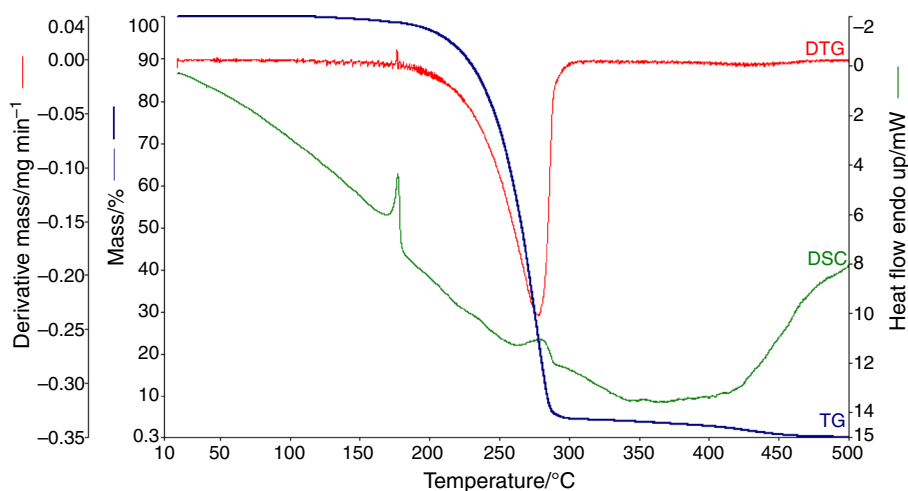**Fig. 6** Thermoanalytical curves for the CPPF compound in air at β = 2 K min^{-1}

Table 3 The thermal effects of CPPF

β/K min^{-1}	Melting temperature range/$^{\circ}$C	Peak maximum/$^{\circ}$C	ΔH_m/kJ mol^{-1}	Endothermic decomposition temperature range/$^{\circ}$C	Peak maximum/$^{\circ}$C	ΔH_d/kJ mol^{-1}
2	173.2–178.9	177.1	27.3	267.6–287.6	280.5	24.4
4	173.4–179.7	177.2	27.0	273.7–295.7	289.4	30.1
6	173.4–180.2	177.3	25.3	278.1–309.8	301.2	36.2
8	174.1–181.2	178.1	28.8	278.2–311.6	302.4	39.6
10	174.6–182.2	178.6	27.2	282.8–314.8	307.4	39.7

of CPPF occurs in two steps: The first step is endothermic and the second step is not accompanied by thermal effect.

Table 3 contains thermophysical and thermochemical properties of melting and oxidative decomposition processes of the CPPF, at five heating rates. Melting and oxidative decomposition enthalpy (ΔH_m and ΔH_d) were calculated using a specialized software, Pyris. They are expressed in kJ mol^{-1}, for the molar mass of 354.5 g mol^{-1} of compound CPPF.

Statistical calculations of data from Table 3 indicate that the melting temperature can be considered the value of 177.66 ± 0.59 °C, the enthalpy of melting can be considered the value of 27.12 ± 1.53 kJ mol^{-1} and the enthalpy of oxidative decomposition may be taken the value of 34.00 ± 5.93 kJ mol^{-1}.

Conclusions

In this study, we present a new azoester dye, 4-(4-chloro-phenyldiazenyl)-2,6-dimethyl-phenyl 2-furoate (CPPF), obtained by condensation of 2-furoyl chloride with 4-(4-chloro-phenylazo)-2,6-dimethyl-phenol in pyridine.

The spectral investigation of the present compound is in agreement with its structure. The UV–Vis spectral analysis shows an intense absorption K-band as a result of the conjugated system Ar–N=N–Ar and a low intensity R-band due to the –N=N– chromophore. The infrared spectrum confirms the presence of azo, carbonyl, and ether groups in the structure of the compound.

The thermal analysis of the azoester demonstrated that it is stable up to 260 °C, melts at 177.66 ± 0.59 °C, and then it decomposes in two steps: the first step is endothermic and the second step is not accompanied by thermal effect.

References

1. Rotaru A, Moanta A, Popa G, Rotaru P, Segal E. Thermal decomposition kinetics of some aromatic azomonoethers. Part IV. Non-isothermal kinetics of 2-allyl-4-[(4-(4-methylbenzyloxy) phenyl)diazenyl] phenol in dynamic air atmosphere. J Therm Anal Calorim. 2009;97:485–91.
2. Rotaru A, Moanta A, Rotaru, Segal E. Thermal decomposition kinetics of some aromatic azomonoethers. Part III. Non-isothermal study of 4-[(4-chlorobenzyl)oxy]-4′-chloro-azobenzene in dynamic air atmosphere. J Therm Anal Calorim. 2009;95:161–6.
3. Rotaru A, Kropidłowska A, Moanta A, Rotaru P, Segal E. Thermal decomposition kinetics of some aromatic azomonoethers. Part II. Non-isothermal study of three liquid crystals in dynamic air atmosphere. J Therm Anal Calorim. 2008;92: 233–38.
4. Rotaru A, Moanta A, Sălăgeanu I, Budrugeac P, Segal E. Thermal decomposition kinetics of some aromatic azomonoethers. Part I. Decomposition of 4-[(4-chlorobenzyl)oxy]-4′-nitro-azobenzene. J Therm Anal Calorim. 2007;87:395–400.
5. Rotaru A, Jurca B, Moanta A, Salageanu I, Segal E. Kinetic study of thermal decomposition of some aromatic ortho-chlorinated azomonoethers. 1.Decomposition of 4[(2-chlorobenzyl)oxi]-4′-trifluoromethyl-azobenzene. Rev Roum Chim. 2006;51:373–8.
6. Moanta A, Ionescu C, Tutunaru B, Dragoi M. Thermal and electron impact decomposition of 4-hydroxy-4′-cyano-azobenzene. Rev Chim Bucharest. 2010;61:657–9.
7. Rotaru A, Constantinescu C, Rotaru P, Moanta A, Dumitru M, Socaciu M, Dinescu M, Segal E. Thermal analysis and thin film deposition by matrix assisted pulsed laser evaporation of a 4 CN type azomonoether. J Therm Anal Calorim. 2008;92:279–84.
8. Moanta A, Ionescu C, Rotaru P, Socaciu M, Harabor A. Structural characterization, thermal investigation and liquid crystalline behavior of 4-[(4-chlorobenzyl)oxy]-3,4′-dichloroazobenzene. J Therm Anal Calorim. 2010;102:1079–86.
9. Moanta A, Tutunaru B, Rotaru P. Spectral and thermal studies of 4-(phenyldiazenyl)phenyl 2-furoate as corrosion inhibitor for carbon steel. J Therm Anal Calorim. 2013;111:1273–9.
10. Moanta A, Samide A, Ionescu C, Tutunaru B, Fruchier A, Barragan-Montero, Dobritescu A. Synthesis and characterization of an azo dye: 4-(phenyldiazenyl)phenyl 2-furoate. Electrochemical and XPS study of its adsorption and inhibitive properties on corrosion of carbon steel in saline water. Int J Electrochem Sci. 2013;8:780–91.
11. Samide A, Tutunaru B, Bratulescu G, Ionescu C. Electrochemical synthesis and characterization of new electrodes based on poly-hematoxylin films. J Appl Polym Sci. 2013;130:687–97.
12. Williams DE, Wright GA. Nucleation and growth of anodic oxide films on bismuth-I. Cycl Voltammetry Electrochim Acta. 1976;21:1009–19.

13. Williams DE. Mechanism of the cathodic reduction of a bismuth oxide anodic film. Electrochim Acta. 1976;21:1097–8.

14. Zerga B, Attayibat A, Sfaira M, Taleb M, Hammouti B, Touhami ME, Radi S, Rais Z. Effect of some tripodal bipyrazolic compounds on C38 steel corrosion in hydrochloric acid solution. J Appl Electrochem. 2010;40:1575–82.

15. Samide A, Tutunaru B. Corrosion inhibition of carbon steel in hydrochloric acid solution using a sulfa drug. Chem Biochem Eng Q. 2011;25:299–308.

16. Samide A, Rotaru P, Ionescu C, Tutunaru B, Moanta A, Barragan-Montero V. Thermal behaviour and adsorption properties of some benzothiazole derivatives. J Therm Anal Calorim. 2014;118:651–9.

17. Rotaru A. Thermal analysis and kinetic study of Petrosani bituminous coal from Romania in comparison with a sample of Ural bituminous coal. J Therm Anal Calorim. 2012;110:1283–91.

18. Constantinescu C, Morîntale E, Emandi A, Dinescu M, Rotaru P. Thermal and microstructural analysis of Cu(II) 2,2′-dihydroxyazobenzene and thin films deposition by MAPLE technique. J Therm Anal Calorim. 2011;104:707–16.

19. Badea M, Olar R, Marinescu D, Segal E, Rotaru A. Thermal stability of some new complexes bearing ligands with polymerizable groups. J Therm Anal Calorim. 2007;88:317–21.

20. Rotaru P, Scorei R, Hărăbor A, Dumitru MD. Thermal analysis of a calcium fructoborate sample. Thermochim Acta. 2010;506:8–13.

21. Tătucu M, Rotaru P, Rău I, Spânu C, Kriza A. Thermal behaviour and spectroscopic investigation of some methyl 2-pyridyl ketone complexes. J Therm Anal Calorim. 2010;100:1107–14.

22. Kocaokutgen H, Gür M, Serkan Soylub M, Lönneckec P. Spectroscopic, thermal and crystal structure properties of novel (E)-2,6-dimethyl-4-(4-tert-butylphenyldiazenyl)phenyl acrylate dye. Dyes Pigments. 2005;67:99–103.

23. Gür M, Kocaokutgen H, Tas M. Synthesis, spectral and thermal characterisation of some azo-ester derivatives containing 4-acryloyloxy group. Dyes Pigments. 2007;72:101–8.

24. Kocaokutgen H, Gumrukcuoglu IE. Thermal characterization of some azo dyes containing intermolecular hydrogen bonds and non-bonds. J Therm Anal Calorim. 2003;71:675–9.

25. Pretsch E, Bühlmann P, Affolter C. Structure determination of organic compounds: tables of spectral data, Berlin: Springer-Verlag; 2000.

26. Astarita A, Cermola F, Iesce MR, Previtera L. Dye-sensitized photooxygenation of sugar furans: novel bis-epoxide and spirocyclic C-nucleosides. Tetrahedron. 2008;64:6744–8.

27. Ewing DF. ^{13}C substituent effects in monosubstituted benzenes. Org Magn Reson. 1979;12:499–524.

28. Rotaru A, Bratulescu G, Rotaru P. Thermal analysis of azoic dyes. Part I non-isothermal decomposition kinetics of [4-(4-chlorobenzyloxy)-3-methylphenyl](p-tolyl)diazene in dynamic air atmosphere. Thermochim Acta. 2009;489:63–9.

29. Rotaru A, Goşa M, Rotaru P. Computational thermal and kinetic analysis. Software for non-isothermal kinetics by standard procedure. J Therm Anal Calorim. 2008;94:367–71.

30. Rotaru A, Goşa M. Computational thermal and kinetic analysis. Complete standard procedure to evaluate the kinetic triplet form non-isothermal data. J Therm Anal Calorim. 2009;97:421–26.